Interface Engineering

DOI: 10.1002/ange.201209816

Revealing Interface-Assisted Charge-Transfer Mechanisms by Using Silicon Nanowires as Local Probes**

Jindong Wang, Zhenxing Wang, Qiaochu Li, Lin Gan, Xinjun Xu, Lidong Li, and Xuefeng Guo**

Charge transfer at the interfaces that are ubiquitous in optoelectronic devices, such as light emitting diodes,[1] field-effect transistors,[2] and organic photovoltaic cells,[3] is of crucial importance to the device performance and stability. Therefore, interface engineering is a general and efficient approach to controlling the doping effects, enhancing the device characteristics, and even installing new functionalities for potential applications in broad areas ranging from integrated circuits and energy conversion to catalysis and chemical/biological sensors.[1–3] Herein, we demonstrate our rational design of building functional semiconductor/environment interfaces, where suspended silicon nanowires (SiNWs) were in direct contact with photoactive titanium oxide quantum dots (TiO_2 QDs; Figure 1), for studying the intrinsic mechanism of interfacial charge trapping/detrapping processes in combination with photoexcitation. SiNWs, as the basic building blocks for semiconductor devices, hold several unique advantages, such as a one-dimensional (1D) nature that maximizes their surface-to-volume ratio, a suitable energy bandgap ($E_g = 1.12$ eV) for high light absorption and efficient charge collection, and easy availability through bottom-up approaches. In conjunction with their superior structural and electrical properties with precise controllability, these form the basis for new types of SiNW-based devices and sensors.[4] Owing to the fact that silicon is the leading material used in today's semiconductor industry, it is natural that 1D SiNWs have become the focus of semiconductor research, as SiNW-based devices have the capability of the integration with the existing silicon industry and processing technology.[5] On the other hand, TiO_2 has been extensively investigated as light antennas owing to its high photoactivity and high resistance to photocorrosion.[6] The unique feature of TiO_2 QDs we want to use in this study is that light irradiation can generate free electrons (e^-) and holes (h^+) as the active centers on the nanoparticle surfaces. Previous reports have demonstrated that these carriers were able to improve the photoactivity of hybrid materials or fine-tune the electrical properties of organic and nanotube-based transistors.[7] Therefore, we propose that the combination of the remarkable optoelectronic properties of SiNWs with the high photoactivity of TiO_2 QDs could provide functional heterojunctions that are able to produce novel functions in optoelectronic devices, such as interesting symmetric mirror-imaging photoswitching with superior rectifying effects in a single SiNW. In fact, the integration of conductive nanomaterials, such as graphenes, nanotubes, and nanowires, with stimuli-responsive components into electrical circuits is an important method to build novel nanoscale devices with desired functionalities that are capable of converting external stimuli to easily detectable electrical signals for potential applications in switching, detecting, and sensing systems.[2b,d,7,8]

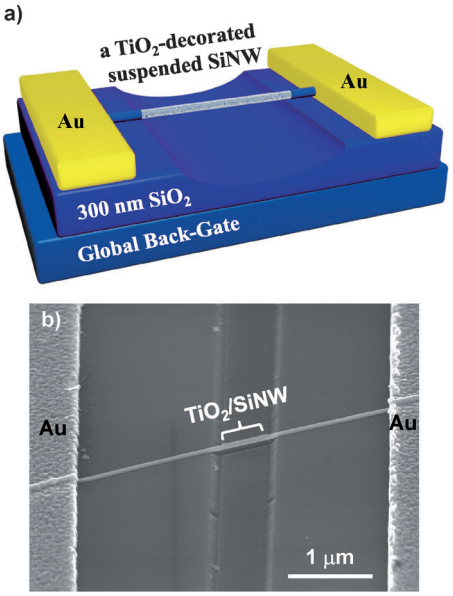

Figure 1. a) Representation of the device structure for TiO_2-decorated suspended individual SiNW transistors. b) SEM image of a suspended SiNW transistor coated by TiO_2 thin films on the trench.

[*] J. Wang,[+] X. Xu, Prof. L. Li
School of Materials Science and Engineering
University of Science and Technology Beijing
Beijing 100083 (P. R. China)
E-mail: lidong@mater.ustb.edu.cn
Z. Wang,[+] Q. Li, L. Gan, Prof. X. Guo
Center for NanoChemistry
Beijing National Laboratory for Molecular Sciences
State Key Laboratory for Structural Chemistry of Unstable and Stable Species
College of Chemistry and Molecular Engineering
Peking University, Beijing 100871 (P. R. China)
E-mail: guoxf@pku.edu.cn
[+] These authors contributed equally to this work.

[**] We thank Yabing Qi (OIST (Japan)) for enlightening discussions. We acknowledge primary financial support from MOST (2012CB921404) and the NSFC (21225311, 51121091, 2112016, 90923015 and 21003002).

Supporting information for this article is available on the WWW under http://dx.doi.org/10.1002/anie.201209816.

TiO_2-decorated suspended individual SiNW transistors (Figure 1) were fabricated as follows. Individual SiNW transistors were first made by electron beam lithography (EBL) on doped silicon wafers with 300 nm of thermally grown SiO_2 on the surface, using SiNWs obtained through a chemical vapor deposition (CVD) process (Supporting Information, Figure S1).[9] Then, we applied another EBL process to open a narrow window well-separated from metal electrodes (500 nm wide and 45 μm long) and subsequent wet etching by a HF solution buffered with NH_4F. In general, SiNWs synthesized by a CVD method have the core–shell nanostructure with the single-crystalline SiNW core that is encircled by an amorphous SiO_2 layer of a few nanometers.[10] This etching step completely removed the amorphous SiO_2 shell exposed in the window. This allows the SiNW core to get in intimate contact with TiO_2 QDs deposited by the following electron beam (e-beam) thermal evaporation. Another important outcome of the etching step is to form a trench by the partial etching of 300 nm SiO_2 on the substrate, thus making SiNWs suspended. It should be mentioned that this fabrication design is very important for ensuring the measurement reliability because of two aspects: one is to maximize the intercommunication between TiO_2 QDs and SiNWs and the other is to rule out potential artifacts from the substrate influence and/or Schottky barrier modification. Finally, we deposited 5 nm-thick TiO_2 thin films through e-beam thermal evaporation before photoresist lift-off to form direct contact interfaces between SiNWs and TiO_2 QDs. The diameters of SiNWs used in this study varied in the range of 60–70 nm (Supporting Information, Figure S2).

SEM (scanning electron microscopy), AFM (atomic force microscopy), and TEM (transmission electron microscopy) were used to characterize the structural properties of the TiO_2/SiNW hybrid architecture (Figure 1 b; Supporting Information, Figures S2a–d), and energy-dispersive X-ray spectroscopy was used to characterize the chemical properties (Supporting Information, Figure S3). The TEM samples were prepared by dispersing SiNWs onto a copper grid from ethanol suspension, then immersing the resulted grid into a buffered HF solution to remove the oxide layer of SiNWs, and finally depositing 5 nm-thick TiO_2 films by e-beam thermal evaporation. According to the energy-dispersive X-ray spectrum, the observation of Ti and Si peaks should result from TiO_2 nanoparticles and SiNWs, respectively, thus demonstrating the chemical composition of TiO_2/SiNW hybrids. We found that TiO_2 thin films consist of numerous TiO_2 nanoparticles with the average diameter of about 10 nm in either anatase or rutile crystalline forms (ca. 1:1; Supporting Information, Figure S2c,d). In the two crystalline forms of TiO_2, rutile is the most stable phase, whereas anatase has the superior optoelectronic and photochemical properties,[6a,11] implying the interesting optoelectronic properties described below.

To confirm the efficiency of TiO_2/SiNW interfaces, we first used p-type SiNWs because of the relative ease of availability. To eliminate possible artifacts from gate hysteresis, all the current–voltage (I–V) curves were collected on the same measurement cycle while scanning from positive to negative bias. The I–V curves obtained from the pristine device exhibited linear transport properties, which indicates the ohmic electrical contacts between SiNWs and metal electrodes (Supporting Information, Figure S4a), with an obvious saturation zone (Supporting Information, Figure S4b). Importantly, all the I–V curves were very stable for a specific SiNW FET under fixed experimental conditions. All of these results set the foundation for the following studies of charge transfer at TiO_2/SiNW interfaces.

After TiO_2 decoration, the devices showed the slight on-state current decrease and the positive shift of the threshold voltage (V_{th}; Supporting Information, Figure S5), which is most likely due to the scattering effect for carriers created by TiO_2 QDs that are in intimate contact with SiNWs and/or chemical doping during device fabrications.[12] Remarkably, these TiO_2-decorated suspended SiNW-based transistors become very sensitive to UV light. UV irradiation experiments were carried out using a handheld UV lamp (254 nm, a low intensity of ca. 50 $\mu W\,cm^{-2}$). We observed two distinct photoswitching behaviors in a single SiNW device when the different source-drain voltages (V_d) were applied. Figure 2

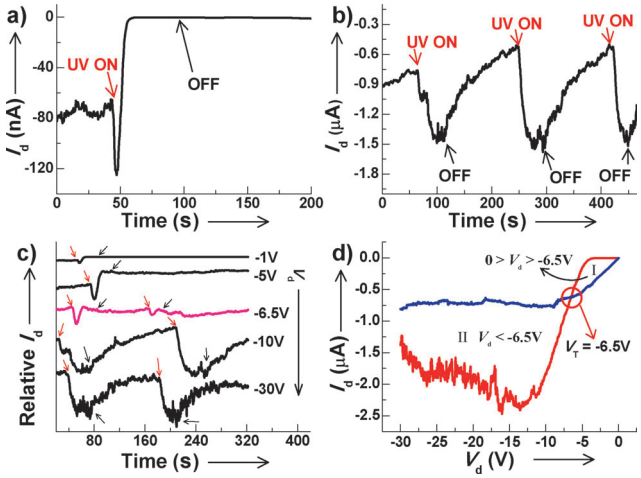

Figure 2. Photoswitching behaviors of a TiO_2-decorated p-type SiNW transistor at different biases. a),b) Time traces of a TiO_2-decorated suspended SiNW transistor at $V_d = -1$ V (a) and $V_d = -10$ V (b) while UV light was toggled on and off. $V_g = -30$ V. c) Time courses of I_d of the same sample at the different V_d. $V_g = -30$ V. Red arrows: UV light on; black arrows: UV light off. d) I–V curves of the same sample before (blue curve) and after (red curve) exposure to UV light at $V_g = -30$ V.

shows such an interesting photoswitching effect when UV light was switched on and off. Noticeably, at a fixed V_d of -1 V ($V_g = -30$ V), we consistently observed an increase of the source-drain current (I_d) at the moment of light turn-on and a gradual decrease of I_d down to the noise level within about 10 seconds; that is, UV irradiation induced the fast transition of I_d from on-state (high conductance) to off-state (low conductance) (Figure 2 a). This implies the existence of different photogenerated competitive mechanisms that control the transition of I_d and thus the device conductance. It is well-accepted that incident UV light generates free electron–hole pairs at the TiO_2/SiNW interfaces.[6] It is unlikely that significant changes in I_d result from Schottky barrier height

modification caused by photoinduced electron–hole pairs at metal-SiNW junctions,[2b,13] because all the devices we used above have the structure where TiO_2 thin films are disconnected with metal electrodes. According to earlier works on photoinduced charge transfer at the semiconductor/insulator interfaces by Calhoun and us,[7a,14] one of the most likely mechanisms is that the photogenerated free electrons at the surface of TiO_2 QDs can migrate to the TiO_2/SiNW interfaces and then behave like a Coulomb trap to quench p-type carriers, thus lowering the carrier mobility in p-type SiNW transistors. This quenching effect can be further enhanced by another possibility that the photogenerated holes at the surface of TiO_2 QDs can photodesorb oxygen molecules from the surface by discharging the surface negative oxygen adsorbates, thus providing the additional free electrons at the interface.[7f,g] To find out more, we performed control experiments using pristine SiNW transistors without TiO_2 decoration. It turned out that these devices showed gradual significant photocurrents when UV light was switched on at the same condition owing to the intrinsic photoresponses of SiNWs (Supporting Information, Figure S6). This is reasonable because silicon has an energy bandgap (E_g) of 1.12 eV that can absorb light efficiently for charge collection.[4c] On the basis of the experimental facts and analysis discussed above, we hypothesize that the opposite effects of the photoactivity of TiO_2 QDs and the intrinsic photoresponsivity of SiNWs on p-type carriers result in the transition of I_d observed above. UV light illumination simultaneously generates fast charge separations in both SiNWs and TiO_2 QDs, which lead to the increase and decrease of I_d, respectively. However, the quenching effect of TiO_2 QDs is relatively slow because the free electrons need a certain time to migrate to the interface and then dominate the influence to the hole carriers that flow through SiNWs. This is why we experimentally first observed the fast increase and then the gradual decrease of I_d at the moment of light turn-on. Interestingly, after UV light was switched off and the devices were kept in the dark, I_d presented a relatively slow relaxation, completing the increase after about 1 hour in this case. This can be explained by the progressive detrapping of holes on the surface of TiO_2 thin films by electrons that originate from the conductive channel where the p-type transistors have a very low density of electrons. In contrast, when a different V_d was used at -10 V while keeping others consistent, we only observed a simple current increase, implying that the intrinsic photoresponses of SiNWs dominate the photoswitching effect in this case (Figure 2b). These photoswitching phenomena are very stable and reproducible as the yield of working devices is very high (15 out of 17 devices).

One important feature of the SiNW photoresponses that should be mentioned is that the photocurrents show a gradual increase with the increase of V_d and then saturate, indicating that the photoinduced charge separation reaches the maximum (Supporting Information, Figure S6). We deduce that this V_d-dependent behavior of the SiNW photoresponses might initiate the intense competition between two mechanisms, as the total amount of the photogenerated electron–hole pairs of TiO_2 QDs remains constant at the same conditions without the obvious voltage-dependence. This may explain the reason why the different mechanism dominates the photoswitching effects at the different source-drain voltage biases observed above. To further prove the hypothesis and abstract more details, we carried out the systematical investigation of the voltage dependence of the photoswitching behaviors in devices. As shown in Figure 2c, by keeping V_g constant, we recorded the time traces of the same device at the different V_d. We did observe the gradual transition of the dominating role from the photoactivity of TiO_2 QDs to the photoresponses of SiNWs with the transition voltage (V_T) of about -6.5 V. When V_d was held at about -6.5 V, the device showed the current equivalent to the original value after the fierce internal contest under UV illumination (pink curve in Figure 2c), indicating that the competition between them reaches equilibrium. Figure 2d shows a comparison of the I–V curves of the same device used above before (blue curve) and after (red curve) exposure to UV light for 45 s. Consistently, we also observed V_T at about -6.5 V. When $0 > V_d > -6.5$ V, the photoactivity of TiO_2 QDs dominates the device photoswitching behavior, thus leading to the current decrease. In contrast, when $V_d < -6.5$ V, the photoresponses of SiNWs play the key role, thus resulting in the current increase. The slight current decrease at high V_d was sometimes observed, which is probably due to the photocurrent stability when the devices were measured under ambient conditions.

The experiments described above consistently prove that TiO_2-decorated suspended SiNW devices show the remarkable V_d-dependence of the photoswitching behavior, thus offering the chance to fine-tune the device performance. Figure 3a shows the comparison of the changes in I_d of another device when the different V_d were applied at a fixed V_g of -30 V. Again, reversible, significant but opposite changes in I_d were observed when V_d was held at -1 V and

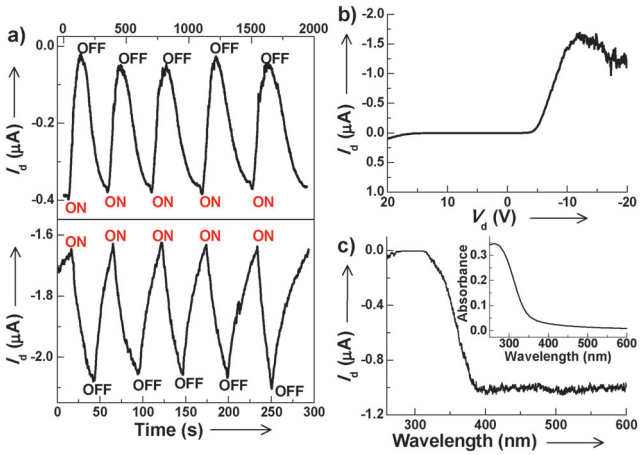

Figure 3. Mirror-imaging photoswitching and rectifying effect of TiO_2-decorated p-type SiNW transistors. a) Time courses of I_d of the same device at different V_d and fixed V_g (-30 V). Top: $V_d = -1$ V; Bottom: $V_d = -10$ V. b) Rectifying effect of the same device at the fixed V_g (-30 V) under UV illumination. c) Wavelength-dependent behavior of another working device. Light was scanned from 250 nm to 600 nm in 5 nm steps with each wavelength left on for 30 s. Inset: the absorption spectrum of 5 nm-thick TiO_2 thin films on quartz substrates. $V_d = -2$ V and $V_g = -30$ V.

−10 V, respectively, in excellent agreement with the phenomena observed above. It is worthwhile to emphasize that rational control of both the photoactivity of TiO_2 QDs and the intrinsic photoresponses of SiNWs realizes symmetric, opposite photoswitching effects, which are effectively mirror images, in a single SiNW-based devices. Another important feature of the system we found is that these functional devices show the reproducible asymmetric *I–V* characteristics behaving like a diode as shown in Figure 3b, thus demonstrating the photocontrollable rectifying effect. This is because the quenching effect of TiO_2 QDs suppresses both the hole carriers in devices and the photoresponses of SiNWs, thus turning off the device conductance at the low $|V_d|$. In most cases, the rectifying effect can be maximized when V_d scans in a large range from positive to negative. Figure 3b presents such a superior rectifying effect of the same device used in Figure 3a when V_d scanned from +20 V to −20 V. The voltage suitable for rectification is very large, from −11 V to +11 V, which is in most part due to asymmetric photoresponses of SiNWs, with the rectification ratio of at least 10^3 at ±11 V. These results strongly suggest that TiO_2-decorated SiNW devices are promising in potential applications in tunable switching and rectifying circuits.[15] To further prove the proposed mechanism, we carried out the wavelength-dependent measurements. As shown in Figure 3c, when light was scanned from 250 nm to 600 nm, the device kept the decreased I_d constant in the range of ≤315 nm and then gradually increased to its saturation at about 390 nm. This behavior is in good agreement with the absorption spectrum of a 5 nm-thick TiO_2 thin film (Figure 3c, inset). Similarly, 254 nm light illumination decreased the device conductance (Supporting Information, Figure S7). This is because 254 nm light (photon energy > TiO_2 QD bandgap > SiNW bandgap) can simultaneously excite both TiO_2 QDs and Si NWs. In contrast, 600 nm light illumination (TiO_2 QD bandgap > photon energy > SiNW bandgap) can only excite Si NWs, thus leading to the consistent increase of I_d (Supporting Information, Figure S8). The slight difference between the wavelength-dependent curve and the absorption spectrum at about 350 nm might originate from the delayed quenching effect because of the slow electron migration to the interface. Furthermore, we also observed that these devices showed power-dependent behavior (Supporting Information, Figure S7).

To summarize the proposed response mechanism, we suggest that the photoexcitation activates the ground-state electrons of both SiNWs and TiO_2 QDs into an excited state. The former increases the carrier density in the conducting channel for charge transport while the latter has the opposite effect by producing active scattering sites at the interface for hole carriers that flow through p-type SiNWs (Figure 4a), thus forming a competitive mechanism with the noticeable bias-dependence. To further understand the mechanism, a possible model of the band bending situation and processes involved at TiO_2/SiNW interfaces is shown in Figure 4b. The photogenerated holes and electrons of TiO_2 QDs at the interface behave differently. The holes are easily trapped inside of TiO_2 nanoparticles, while the electrons can migrate to the interface.[7e,16] Under a negative gate bias, the electrons move toward the semiconductor/dielectric interface and behave like a Coulomb trap to lower the hole-carrier mobility in the p-type semiconductors.

On the basis of deep understanding of the intrinsic charge transfer mechanism, it can be rationally inferred that we should observe only the current increase when an n-type SiNW is used. To test this prediction, we followed the same device fabrication procedure to make TiO_2-decorated sus-

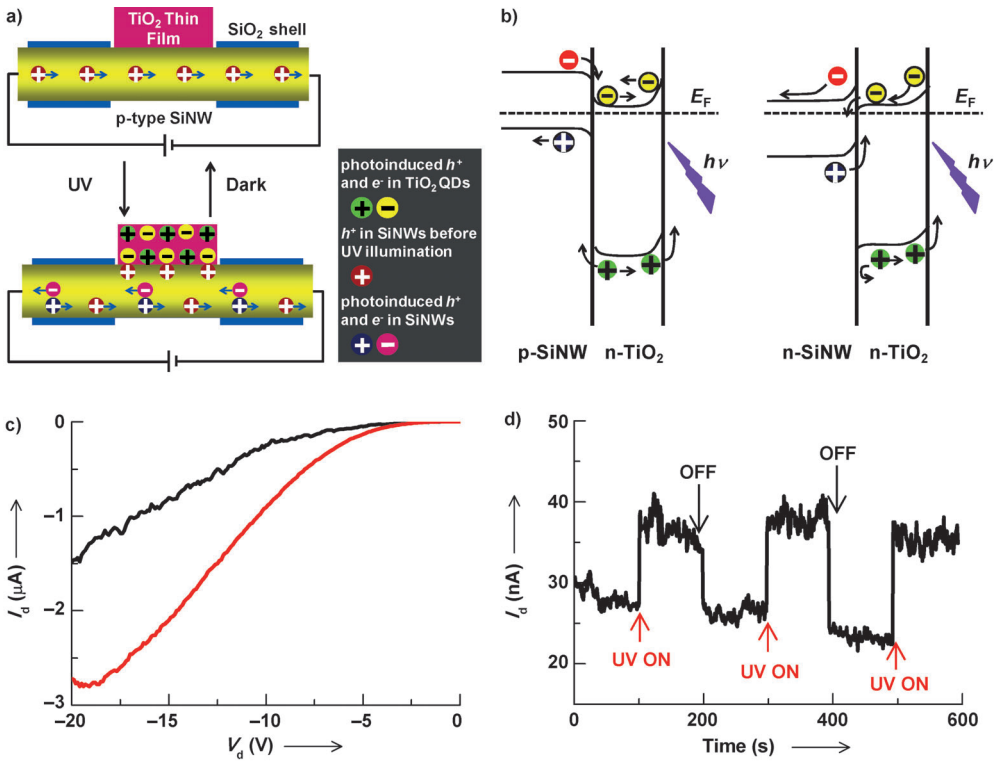

Figure 4. Competitive photoswitching mechanisms of TiO_2-decorated SiNW transistors. a) Mechanism illustration of charge transfer at TiO_2/SiNW interfaces upon exposure to UV light. b) Energy-level diagrams of TiO_2/p-SiNW and TiO_2/n-SiNW junctions. c) *I–V* curves of TiO_2-coated individual n-type SiNW devices before (black) and after (red) exposure to UV light at $V_g = -20$ V. d) Time courses of I_d of the same device at $V_d = -6$ V and $V_g = -20$ V.

pended n-type SiNW devices (Supporting Information, Figure S9). As expected, we did not observe the transition of I_d from the low-conductance state to the high-conductance state at any V_d biases (Figure 4c). This is reasonable because the photoinduced free electrons of TiO_2 QDs can scatter the hole carriers in a p-type semiconductor and have an opposite function as active excitons to increase the electron current in a n-type material. Therefore, the synergetic effects of the photoactivity of TiO_2 QDs and the intrinsic photoresponses of SiNWs lead to the consistent current increase of the devices. Compared with those in p-type devices, the photoswitching effect in these n-type devices shows the quicker detrapping process (Figure 4d). This is because electrons expected to recombine trapped holes on the surface of TiO_2 nanoparticles originate from the conductive channel of the n-type transistors that have the much higher electron density. It is interesting to mention that the combination of the complementary photoresponsive behaviors of both n-type and p-type SiNWs should afford another remarkable example of mirror-imaging photoswitching effects.

In summary, this study described a straightforward method to reveal intrinsic charge transfer mechanisms at the semiconductor/environment interfaces using SiNWs as local probes in combination with photoexcitation. In general, UV irradiation activates the ground-state electrons of both SiNWs and TiO_2 QDs into an excited state. The former increases the carrier density in the conducting channel for both p-type and n-type SiNWs, while the latter has different behavior. In a p-type SiNW, the photoinduced free electrons of TiO_2 QDs produce active scattering sites at the interface for hole carriers and lower the carrier mobility, thus forming a competitive mechanism with the noticeable bias-dependence. Remarkably, rational utility of deep mechanism understanding leads to realizing mirror-imaging photoswitching and tunable rectifying effects in a single SiNW-based device. In contrast, in an n-type SiNW, these free electrons have the opposite effect, thus working synergistically with the former mechanism to afford the consistent current increase in devices. The concept of interface engineering demonstrated in this study should provide new insights into designing novel interfaces for studying the intrinsic mechanism of interface phenomena to elucidate the interplay among parameters that control charge separation, charge recombination, charge transfer, and properties of optoelectronic devices.

Received: December 8, 2012
Revised: January 26, 2013
Published online: February 11, 2013

Keywords: charge trapping/detrapping · photoswitching · silicon nanowires · titanium dioxide

[1] a) J. Zaumseil, H. Sirringhaus, *Chem. Rev.* **2007**, *107*, 1296 – 1323; b) S. R. Forrest, *Chem. Rev.* **1997**, *97*, 1793 – 1896.

[2] a) F. Patolsky, G. F. Zheng, C. M. Lieber, *Anal. Chem.* **2006**, *78*, 4260 – 4269; b) S. Liu, Q. Shen, Y. Cao, L. Gan, Z. X. Wang, M. L. Steigerwald, X. F. Guo, *Coord. Chem. Rev.* **2010**, *254*, 1101 – 1116; c) C. A. Di, Y. Q. Liu, G. Yu, D. B. Zhu, *Acc. Chem. Res.* **2009**, *42*, 1573 – 1583; d) W. R. Yang, K. R. Ratinac, S. P. Ringer, P. Thordarson, J. J. Gooding, F. Braet, *Angew. Chem.* **2010**, *122*, 2160 – 2185; *Angew. Chem. Int. Ed.* **2010**, *49*, 2114 – 2138; e) A. Facchetti, M. H. Yoon, T. J. Marks, *Adv. Mater.* **2005**, *17*, 1705 – 1725.

[3] J. L. Brédas, J. E. Norton, J. Cornil, V. Coropceanu, *Acc. Chem. Res.* **2009**, *42*, 1691 – 1699.

[4] a) T. J. Kempa, B. Z. Tian, D. R. Kim, J. S. Hu, X. L. Zheng, C. M. Lieber, *Nano Lett.* **2008**, *8*, 3456 – 3460; b) B. Z. Tian, X. L. Zheng, T. J. Kempa, Y. Fang, N. F. Yu, G. H. Yu, J. L. Huang, C. M. Lieber, *Nature* **2007**, *449*, 885 – 888; c) R. X. Yan, D. Gargas, P. D. Yang, *Nat. Photonics* **2009**, *3*, 569 – 576; d) D. R. Kim, C. H. Lee, X. L. Zheng, *Nano Lett.* **2009**, *9*, 1984 – 1988; e) B. Z. Tian, T. Cohen-Karni, Q. Qing, X. J. Duan, P. Xie, C. M. Lieber, *Science* **2010**, *329*, 830 – 834.

[5] a) Y. Y. Wu, R. Fan, P. D. Yang, *Nano Lett.* **2002**, *2*, 83 – 86; b) Y. Huang, X. F. Duan, C. M. Lieber, *Small* **2005**, *1*, 142 – 147; c) M. C. McAlpine, H. D. Agnew, R. D. Rohde, M. Blanco, H. Ahmad, A. D. Stuparu, W. A. Goddard, J. R. Heath, *J. Am. Chem. Soc.* **2008**, *130*, 9583 – 9589; d) K. Q. Peng, X. Wang, X. L. Wu, S. T. Lee, *Nano Lett.* **2009**, *9*, 3704 – 3709; e) C. B. Winkelmann, I. Ionica, X. Chevalier, G. Royal, C. Bucher, V. Bouchiat, *Nano Lett.* **2007**, *7*, 1454 – 1458; f) Y. Wu, J. Xiang, C. Yang, W. Lu, C. M. Lieber, *Nature* **2004**, *430*, 61 – 65; g) P. Zhang, X. T. Zhou, Y. H. Tang, T. K. Sham, *Langmuir* **2005**, *21*, 8502 – 8508.

[6] a) A. Fujishima, X. T. Zhang, D. A. Tryk, *Surf. Sci. Rep.* **2008**, *63*, 515 – 582; b) M. R. Hoffmann, S. T. Martin, W. Y. Choi, D. W. Bahnemann, *Chem. Rev.* **1995**, *95*, 69 – 96.

[7] a) M. F. Calhoun, C. Hsieh, V. Podzorov, *Phys. Rev. Lett.* **2007**, *98*, 096402; b) S. Liu, J. M. Li, Q. Shen, Y. Cao, X. F. Guo, G. M. Zhang, C. Q. Teng, J. Zhang, Z. F. Liu, M. L. Steigerwald, D. S. Xu, C. Nuckolls, *Angew. Chem.* **2009**, *121*, 4853 – 4856; *Angew. Chem. Int. Ed.* **2009**, *48*, 4759 – 4762; c) J. Yoon, S. Cho, J. H. Kim, J. Lee, Z. X. Bi, A. Serquis, X. H. Zhang, A. Manthiram, H. Y. Wang, *Adv. Funct. Mater.* **2009**, *19*, 3868 – 3873; d) Y. J. Hwang, A. Boukai, P. D. Yang, *Nano Lett.* **2009**, *9*, 410 – 415; e) Q. Shen, Y. Cao, S. Liu, L. Gan, J. M. Li, Z. X. Wang, J. S. Hui, X. F. Guo, D. S. Xu, Z. F. Liu, *J. Phys. Chem. Lett.* **2010**, *1*, 1269 – 1276; f) J. An, K. Xue, W. G. Xie, Q. Li, J. B. Xu, *Nanotechnology* **2011**, *22*, 135702; g) S. Liu, J. F. Ye, Y. Cao, Q. Shen, Z. F. Liu, L. M. Qi, X. F. Guo, *Small* **2009**, *5*, 2371 – 2376.

[8] a) X. L. Li, Y. Jia, A. Y. Cao, *ACS Nano* **2010**, *4*, 506 – 512; b) Y. F. Li, T. Kaneko, J. Kong, R. Hatakeyama, *J. Am. Chem. Soc.* **2009**, *131*, 3412 – 3413; c) Y. Lin, K. Zhang, W. F. Chen, Y. D. Liu, Z. G. Geng, J. Zeng, N. Pan, L. F. Yan, X. P. Wang, J. G. Hou, *ACS Nano* **2010**, *4*, 3033 – 3038; d) F. Patolsky, B. P. Timko, G. H. Yu, Y. Fang, A. B. Greytak, G. F. Zheng, C. M. Lieber, *Science* **2006**, *313*, 1100 – 1104; e) Y. L. Zhao, J. F. Stoddart, *Acc. Chem. Res.* **2009**, *42*, 1161 – 1171.

[9] a) W. I. Park, G. F. Zheng, X. C. Jiang, B. Z. Tian, C. M. Lieber, *Nano Lett.* **2008**, *8*, 3004 – 3009; b) F. Patolsky, G. F. Zheng, C. M. Lieber, *Nat. Protoc.* **2006**, *1*, 1711 – 1724.

[10] Y. Cui, L. J. Lauhon, M. S. Gudiksen, J. F. Wang, C. M. Lieber, *Appl. Phys. Lett.* **2001**, *78*, 2214 – 2216.

[11] C. Wu, L. Lei, X. Zhu, J. Yang, Y. Xie, *Small* **2007**, *3*, 1518 – 1522.

[12] D. Zhang, L. Gan, Y. Cao, Q. Wang, L. Qi, X. Guo, *Adv. Mater.* **2012**, *24*, 2715 – 2720.

[13] a) P. G. Collins, K. Bradley, M. Ishigami, A. Zettl, *Science* **2000**, *287*, 1801 – 1804; b) R. J. Chen, N. R. Franklin, J. Kong, J. Cao, T. W. Tombler, Y. G. Zhang, H. J. Dai, *Appl. Phys. Lett.* **2001**, *79*, 2258 – 2260.

[14] Q. Wang, X. F. Guo, L. C. Cai, Y. Cao, L. Gan, S. Liu, Z. X. Wang, H. T. Zhang, L. D. Li, *Chem. Sci.* **2011**, *2*, 1860 – 1864.

[15] C. Liu, Y. J. Hwang, H. E. Jeong, P. Yang, *Nano Lett.* **2011**, *11*, 3755 – 3758.

[16] T. Dittrich, V. Duzhko, F. Koch, V. Kytin, J. Rappich, *Phys. Rev. B* **2002**, *65*, 155319.

